3D-Orientation Space; Filters and Sampling

Frank G.A. Faas* and Lucas J. van Vliet

Pattern Recognition Group, Delft University of Technology,
Lorentzweg 1, 2628 CJ, Delft, The Netherlands,
{faas,lucas}@ph.tn.tudelft.nl

Abstract. The orientation space transform is a concept that can deal with multiple oriented structures at a single location. In this paper we extend the orientation space transform to 3D images producing a 5D orientation space (x, y, z, ϕ, θ). We employ a tunable, orientation selective quadrature filter to detect edges and planes and a separate filter for detecting lines. We propose a multi-resolution sampling grid based on the icosahedron. We also propose a method to visualize the resulting 5D space. The method can be used in many applications like (parametric) curve and plane extraction, texture characterization and curvature estimation.

1 Introduction

Three-dimensional images can be seen as compositions of numerous simple structures like planes, textures, edges and lines. Therefore multiple oriented structures can be present at a single point. Here we will describe a method which can deal with such occurrences in 3D. Detectors developed in the past, like the tensor approach [2,3,8], can handle single oriented structures but often fail on non-isolated structures. Therefore we present a multi orientation analysis as first proposed by [12] and later implemented in 2D by e.g.[6]. In our multi-orientation analysis, we probe to see how much oriented structure is present that exhibits the probe orientation. We filter the image with rotated versions of an orientation-selective template filter m and stack the accumulated evidence in two extra angular dimensions

$$I_m(\boldsymbol{x}, \phi, \theta) = I(\boldsymbol{x}) * m(\boldsymbol{x}; \phi, \theta). \tag{1}$$

Here $\boldsymbol{x}$ contains the spatial dimensions, x, y and z. The template orientation is given by ϕ and θ. With ϕ the counterclockwise angle in the xy-plane measured from the positive x-axis, ranging from 0 to 2π, and θ measures the angular distance from the positive z-axis, with θ ranging from 0 to π. The asterisk denotes the convolution operator.
Now let us define orientation for line and plane-like structures. When we draw a line through the center of a unit sphere we will find two intersection points.

* This work was partially supported by Rolling Grants program 94RG12 of the Netherlands Organization for Fundamental Research of Matter (FOM).

J. Bigun and T. Gustavsson (Eds.): SCIA 2003, LNCS 2749, pp. 36–42, 2003.

These points can be specified by their respective θ and ϕ coordinates. Both pairs of $\{\theta, \phi\}$-coordinates can be used as orientation but to avoid ambiguities we have to drop one pair. So let us now define the orientation of a line as the pair of coordinates for which: $\theta \in [0, \pi/2\rangle$ or $\theta = \pi/2 \wedge \phi \in [0, \pi\rangle$. For a plane we adopt the same formulation in which the line is replaced by the normal to the plane.
Note that this coordinate representation contains discontinuities due to the fact that ϕ and $(\pi/2 - \theta)$ are modulo 2π and $\pi/2$ respectively. However these discontinuities pose no problems for further filtering as they are coordinate discontinuities which can be easily dealt with by applying a standard boundary extension technique. This in contrast to the tensor approach in which the filter output is discontinuous, the output therefore has to be remapped for further processing in most cases [7].
Further we will show a few ways of visualizing the results of the orientation space transform.

2 3D-Orientation Space: Filter Design

In designing our filters the first thing to realize is the trade-off between orientation selectivity and localization. By increasing the orientation selectivity the filter becomes more extended and loses localization, i.e. the filter response changes slowly along the long axes of the filter. We want to treat the orientation and scale selectivity separately, therefore the filter is made polar separable in Fourier space, see e.g. [9],

$$\mathcal{F}\{m\}(\boldsymbol{f}; \phi_i, \theta_i) = M_{rad}(f)\, M_{ang}(\phi, \theta; \phi_i, \theta_i) \qquad \text{with } f = |\boldsymbol{f}|. \tag{2}$$

With $\boldsymbol{f} = (f, \phi, \theta)$ the spherical coordinates in Fourier space. Now the radial function specifies the scale and the angular part the selectivity of the filter. Proper sampling and discretization of the resulting orientation space require that the input image, as well as the filters, are band-limited. For correct sampling along the ϕ and θ axes the filters should be radial and angular band-limited [5, 6].
In 2D, lines and edges can be treated equally using quadrature filters. In 3D, there is a similar relation between edges and planes. However the line appears as a new structure which requires separate treatment and has no associated quadrature structure. Therefore we design two filters, one for line like structures and a quadrature filter for planar structures. Furthermore the 3D filters used are generalizations of a 2D filter presented in [6, Chap. 3].
The angular part of the filters is defined as:

$$M_{ang}(\phi, \theta; \phi_i, \theta_i) = M(\boldsymbol{f}, \boldsymbol{\psi_i}) = 2e^{-\frac{1}{2}\frac{\rho^2}{\sigma_s^2}}, \tag{3}$$

where

$$\rho = \begin{cases} \angle(\boldsymbol{f}, \boldsymbol{\psi_i}) & \text{plane filter(spatial)} \\ \pi/2 - \angle(\boldsymbol{f}, \boldsymbol{\psi_i}) & \text{line filter(spatial),} \end{cases} \tag{4}$$

with

$$\boldsymbol{\psi_i} = \begin{pmatrix} \cos(\phi_i)\sin(\theta_i) \\ \sin(\phi_i)\sin(\theta_i) \\ \cos(\theta_i) \end{pmatrix}, \tag{5}$$

and

$$\sigma = 2\arccos(1 - 2/N). \tag{6}$$

The orientation selectivity σ is found by equating the surface area of the unit hemi-sphere, $S = 2\pi$, with N times the area S_{cone}. Here S_{cone} is given by the intersection of S with a solid cone with opening angle σ. In this formulation the orientation selectivity can be increased by raising N and the sampling distance is approximately 1σ as required by band-limiting the Gaussian [11, Chap. 2]. The quadrature structure for the planar filter only requires that the filter is zero for $\rho > \pi/2$, this is approximately satisfied, as for $N \geq 15$ the 3σ radius lies well within $\pi/2$. Now let us define the radial part of the filter [6],

$$M_{rad} = \left(\frac{f}{f_c}\right)^{\left(\frac{f_c}{b_f}\right)^2} e^{-\left(\frac{f^2 - {f_c}^2}{2{b_f}^2}\right)} \tag{7}$$

This Gaussian-like function has a bandwidth b_f and an central frequency f_c. An advantage of this filter over a true Gaussian of bandwidth b_f and center frequency f_c is a guaranteed zero response to constant signals. The resulting plane filter has a droplet shape and the line filter has a donut shape as footprint in Fourier space.

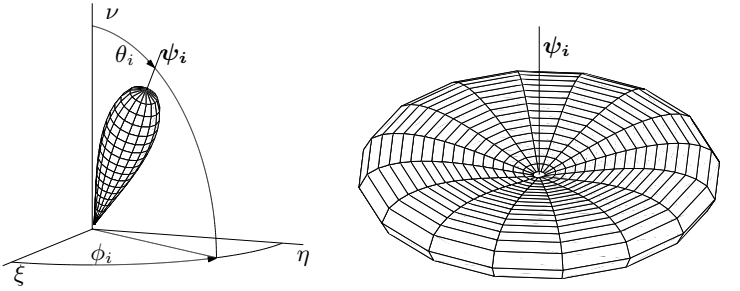

a. b.

Fig. 1. (a) Planar quadrature filter M_i , with ξ, η and ν the Cartesian Fourier coordinates and filter orientation angles $\{\phi_i, \theta_i\}$. (b) The same as (a) but for the line filter. The parameters used for these filters: $f_c = 0.2$, $b_f = 0.16$.

3 3D-Orientation Space: Sampling Grid

Sampling the orientation space by N samples requires filtering image $I(\boldsymbol{x})$ with N rotated copies of an elongated template filter m, such that its principle axis

coincides with orientation $\{\phi_i, \theta_i\}$. The result, $I_m(\boldsymbol{x}, \phi_i, \theta_i)$ is a 5D-orientation space. Now let us look at how to distribute the N orientations, $\boldsymbol{\psi_i}$ over one hemisphere, i.e. here the upper half of the unit sphere. We only need to address the upper half as we cannot distinguish between opposite directions.
Ideally the angular distance from each point to its direct neighbors should be constant, at least for 3D volume images like those acquired with MRI. But in cases where the human perception is mimicked this is does not hold, e.g. our perception of speed is not uniform across spatial frequencies [1]. As there is no general solution for the problem of distributing a set of points equidistant over a sphere [10], we have adopted a grid based on the icosahedron inspired by [4]. The icosahedron is the largest of the platonic solids and has 20 identical faces consisting of equilateral triangles and 12 vertices, Fig. 2.a and b. On each of the faces we impose a hexagonal grid. This grid is then projected on the unit sphere to obtain the orientations (Fig. 2). This pixelization scheme is symmetric in the origin and allows easy indexation (addressing). We can easily change the number of points by imposing a finer/courser hexagonal grid on the faces of the icosahedron. The number of points is given by $N = 5n^2 - 10n + 6$ with n the number of points on a single side of a face ($n \geqq 2$). Furthermore the grid is hexagonal with the exception of the vertex-points of the icosahedron which are pentagonal. Points are indexed with three indices as shown in Fig. 2.b. Index F denotes a strip of 4 faces while I and J are subindices on this strip. Note that the points on the border of the strip should be treated differently to avoid multiple indexation of a single orientation. This scheme allows us to easily find the neighboring orientations which is useful for connectivity issues.

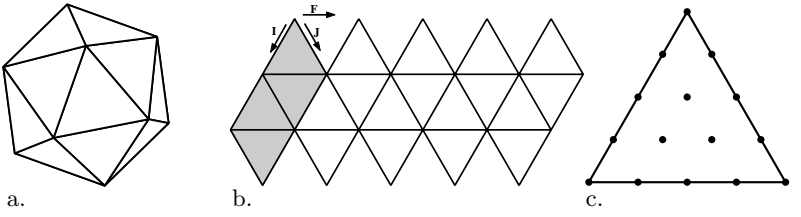

Fig. 2. (a) Icosahedron, platonic solid with largest number of faces. (b) Unfolded icosahedron. (c) Hexagonal grid at one face of the icosahedron

4 Test Experiments and Visualization

Now let us look how we can visualize orientation space. Therefore we investigate a simple image of a fork structure constructed from three line segments with a Gaussian profile of 1σ (Fig. 3.a). The image size is 75^3 voxels and the parameters used for calculating the orientation space are (f_c,b_f,N)=(0.2,0.16,181). Figures 3.b-d show isosurfaces of the response of three filters on the fork image, where the tree filters are those with the highest responses. As can be seen the orientation

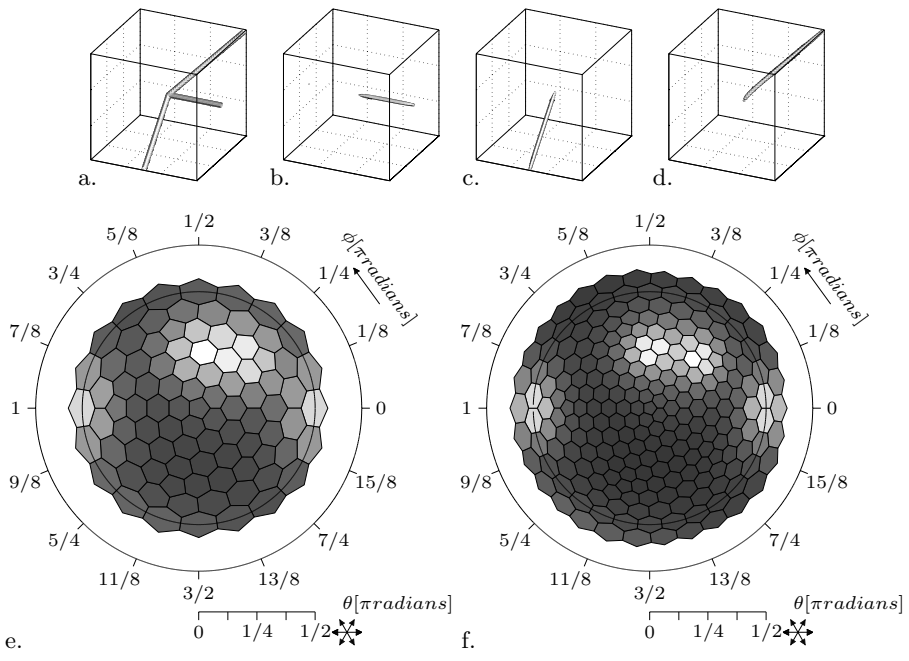

Fig. 3. (a) isosurface of a fork-structure with a size of 75^3 voxels. (b-d) isosurface of $I_m(\boldsymbol{x}, \phi_c, \theta_c)$ for the three orientations c, with the highest responses.(e-f) Polar voronoi diagrams of the voxel closest to the intersection point of the three line segments for an orientation space of respectively 81 and 181 sample orientations.

space response is smooth and contains local orientation information. To use orientation space for segmenting the image, the oriented structures which are in this case line segments, should be resolved. Now we assume two structures can be resolved if the minimum response between the two is less than half the maximum response. This states that the minimum angle between the oriented structures must be larger than $4\sqrt{\ln 2}\sigma$ according to [6]. As the minimum angle of separation in our image is 35° the minimum number of sampling orientations required is 140. Now we will show the output of two angular resolutions with respectively 81 and 181 sampling orientations. Let us inspect the angular responses of these two spaces for the center voxel where the three line segments meet. In Fig. 3.e-f we show two polar voronoi plots of the angular response of the two orientation spaces. A voronoi cell is defined as the set of orientations closer to $\boldsymbol{\phi}_i$ than to all other $\boldsymbol{\phi}_{j\neq i}$. In the plot each voronoi cell has a gray value corresponding to the height of the orientation space response. In the plot, θ is the radial and ϕ the angular coordinate. Orientation (ϕ, θ)=(0,0) can be found in the center of the plot and orientations with $\theta = \pi/2$ can be found on the inner solid circle. In Fig. 3.e we can see three peaks. But the two peaks centered around (0,π/2) and (0,3/2π) belong to one and the same orientation since a line through the center of a sphere yields two crossings at opposite sides. More interesting is the

other peak with the elliptical shape. This shape indicates that the underlying structure(s) are not resolved, as predicted by the angular resolution criterion. In Fig. 3.f the number of sampling orientations is increased from 81 to 181. As can be seen the responses of the two lines are now nicely resolved. Therefore, only the orientation space with 181 sampling points can be used to segment the fork image.

Now let us look at another visualization method for a 5D orientation space. In Fig. 4.a we show an image with a line through its center. In Fig. 4.b we plot the orientation space (46 sample orientations) of the 27 voxels in the center of the image. On the individual spheres the voronoi cells are plotted in the same way as for the polar voronoi plot. With orientation $\{\phi, \theta\} = \{0, 0\}$ on top of the spheres and all spheres rotated through an angle π around the ϕ-axis. In the image we see that the response is localized and drops off very quickly with the distance to the line. It is actually possible to prove it has a Gaussian profile.

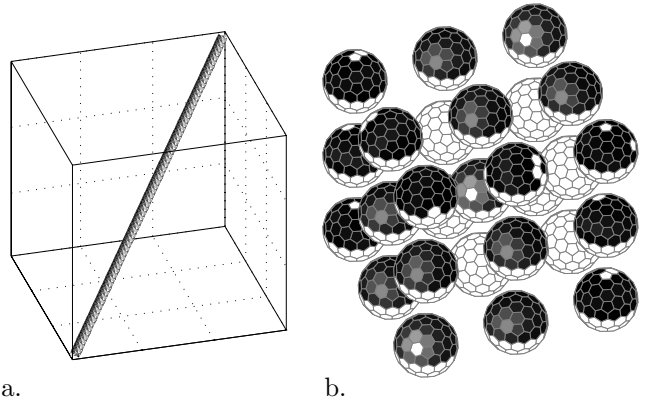

a. b.

Fig. 4. (a) isosurface of a Gaussian line. (b) the corresponding 5D orientation space of the 27 center voxels of the image in (a).

5 Conclusions

We have extended the principle of orientation space to 3D images by designing orientation selective line and plane/edge filters. After an elaborate search for sampling grids on a sphere we selected a multi-scale grid based on the icosahedron which allows easy addressing. We presented methods to visualize the resulting 5D structure. The method can deal with multiple intersecting oriented structures and contains local orientation information. In the future we will try to produce an orientation space formulation which is sparse and local. This to limit the computational burden and memory consumption. Further we will investigate some interesting applications of the orientation space approach.

References

1. J. Bigün. Speed, frequency, and orientation tuned 3-d gabor filterbanks and their design. In *Proceedings of International Conference on Pattern Recognition, ICPR, Jerusalem*, pages C–184–187. IEEE Computer Society.
2. J. Bigün and G. H. Granlund. Optimal Orientation Detection of Linear Symmetry. In *First International Conference on Computer Vision, ICCV (London)*, pages 433–438. IEEE Computer Society Press, June 8–11 1987.
3. J. Bigün, G.H. Granlund, and J. Wiklund. Multidimensional orientation estimation with applications to texture analysis and optical flow. *IEEE Transaction on Pattern Analysis and Machine Intelligence*, 13(8):775–790, 1991.
4. L. Dorst. A coordinate system for the crystal ball. Technical report, Delft University of Technology, 1980.
5. W.T. Freeman and E.H. Adelson. The design and use of steerable filters. *IEEE Transactions on Pattern Analysis and Machine Intelligence*, 13(9):891–906, September 1991.
6. M. van Ginkel. *Image Analysis using Orientation Space based on Steerable Filters.* PhD thesis, Delft University of Technology, Delft, The Netherlands, 2002.
7. H. Knutsson. Producing a continuous and distance preserving 5-d vector representation of 3-d orientation. In *IEEE Computer Society Workshop on Computer Architecture for Pattern Analysis and Image Database Management*, pages 175–182. Miami Beach, Florida, November 18–20 1985.
8. H. Knutsson. Representing local structure using tensors. In *The 6th Scandinavian Conference in Image Analysis*, pages 244–251, Oulu, Finland, June 19–22 1989.
9. H. Knutsson and G. H. Granlund. Fourier domain design of line and edge detectors. In *Proceedings of the 5th International Conference on Pattern Recognition*, Miami, Florida, December 1980.
10. E.B. Saff and A.B.J. Kuijlaars. Distributing many points on a sphere. *the Mathematical Intelligencer*, 19(1):5–11, 1997.
11. L.J. van Vliet. *Grey-Scale Measurements in Multi-Dimensional Digitized Images.* PhD thesis, Delft University of Technology, Delft, The Netherlands, October 1993.
12. D. Walters. Selection of image primitives for general-purpose visual processing. *Computer Vision, Graphics, and Image Processing*, 37:261–298, 1987.